


Article

Climate Change Impacts on Crop Yield of Winter Wheat (*Triticum aestivum*) and Maize (*Zea mays*) and Soil Organic Carbon Stocks in Northern China

Chuang Liu ^{1,2}, Huiyi Yang ^{2,†}, Kate Gongadze ^{2,‡}, Paul Harris ² , Mingbin Huang ³  and Lianhai Wu ^{2,*} 

- ¹ Key Laboratory of Nutrient Cycling Resources and Environment of Anhui, Institute of Soil and Fertilizer, Anhui Academy of Agricultural Sciences, Hefei 230001, China; liuchuang@aaas.org.cn
- ² Rothamsted Research, North Wyke, Okehampton, Devon EX20 2SB, UK; h.yang@greenwich.ac.uk (H.Y.); kate.gongadze@bristol.ac.uk (K.G.); paul.harris@rothamsted.ac.uk (P.H.)
- ³ State Key Laboratory of Soil Erosion and Dryland Farming on the Loess Plateau, Institute of Soil and Water Conservation, Northwest A&F University, Xianyang 712100, China; hmdb@nwsuaf.edu.cn
- * Correspondence: lianhai.wu@rothamsted.ac.uk
- † Current address: Natural Resources Institute, Faculty of Engineering & Science, University of Greenwich, Chatham Maritime, Kent ME4 4TB, UK.
- ‡ Current address: Department of Aerospace Engineering, University of Bristol, Cantock's Close, Bristol BS8 1TS, UK.

Abstract: Agricultural system models provide an effective tool for forecasting crop productivity and nutrient budgets under future climate change. This study investigates the potential impacts of climate change on crop failure, grain yield and soil organic carbon (SOC) for both winter wheat (*Triticum aestivum* L.) and maize (*Zea mays* L.) in northern China, using the SPACSYS model. The model was calibrated and validated with datasets from 20-year long-term experiments (1985–2004) for the Loess plateau, and then used to forecast production (2020–2049) under six sharing social-economic pathway climate scenarios for both wheat and maize crops with irrigation. Results suggested that warmer climatic scenarios might be favourable for reducing the crop failure rate and increasing the grain yield for winter wheat, while the same climatic scenarios were unfavourable for maize production in the region. Furthermore, future SOC stocks in the topsoil layer (0–30 cm) could increase but in the subsoil layer (30–100 cm) could decrease, regardless of the chosen crop.

Keywords: SPACSYS; crop failure; soil organic carbon; modelling; Loess



Citation: Liu, C.; Yang, H.; Gongadze, K.; Harris, P.; Huang, M.; Wu, L. Climate Change Impacts on Crop Yield of Winter Wheat (*Triticum aestivum*) and Maize (*Zea mays*) and Soil Organic Carbon Stocks in Northern China. *Agriculture* **2022**, *12*, 614. <https://doi.org/10.3390/agriculture12050614>

Academic Editor: Rosa Francaviglia

Received: 11 March 2022

Accepted: 24 April 2022

Published: 26 April 2022

Publisher's Note: MDPI stays neutral with regard to jurisdictional claims in published maps and institutional affiliations.



Copyright: © 2022 by the authors. Licensee MDPI, Basel, Switzerland. This article is an open access article distributed under the terms and conditions of the Creative Commons Attribution (CC BY) license (<https://creativecommons.org/licenses/by/4.0/>).

1. Introduction

Climate change poses a great challenge to worldwide agriculture production [1,2], where warmer temperatures greatly accelerate soil evaporation, which in turn increases drought severity, especially in the world's drier regions where plant growth and development depend on water availability [3,4]. Further, crop yield will become increasingly unstable [1] with increases in crop failure rates [5]. For example, excess and uneven distributions of rainfall could lead to a substantial decline in maize yield [6] where frequent heavy rainfall events over crop flowering and grain-filling periods will increase nitrogen (N) losses through leaching and runoff [7]. Conversely, an increase in atmospheric CO₂ concentration can stimulate plant photosynthetic carbon (C) fixation, which indirectly mitigates adverse impacts of climate change [8–10]. Thus, both pros and cons of climate change to agricultural production have to be considered for implementing positive adaptation strategies.

Soil organic carbon (SOC) is a critical element for crop production and acts as an important determinant for climate change where SOC is subject to inter-annual variability due to changes in agronomic practice and meteorological cycles [11,12]. Climate change can increase dissolved C loss through runoff, which reduces soil productivity by increases in soil erosion risk and soil fertility degradation [13,14]. In addition, the C input to soils from

crops is incorporated into the SOC pool, which increases its complexity due to processes of decomposition and stabilisation [15]. Northern China is a major agricultural region in China, especially for winter wheat (*Triticum aestivum* L.) and maize (*Zea mays* L.) but is vulnerable to the impacts of climate change [16] leading to social and economic instability nationally and potentially, globally [17,18]. Thus, elucidating the relationship between climate change and crop yield and SOC stock is critically important for agricultural production and food security, not only in the region, but for impacts further afield also.

Although the statistical analyses of measured data can reveal the impacts of real-time meteorological variables and controlled variables on crop yield and SOC stock, it is effectively impossible to monitor the impacts of different climatic scenarios in the future through data-driven models. In this respect, agricultural system (mathematical) models provide a valuable tool for simulating (predicting) future crop productivity and nutrient cycling under different agronomic practices and climate change scenarios [19]. The SPACSYS (Soil-Plant-Atmosphere-Continuum SYStem) model is one such process-based model and is capable of simulating processes in plant growth, C, N and phosphorus (P) cycling, water redistribution and heat transformation [20–22], together with more recent functionality in simulating ruminant animal growth [23]. SPACSYS has been used to assess the effects of climate change on crop yield, N losses, greenhouse gas (GHG) emissions and soil C and N stocks with different cropping systems across different climatic regions [7,21,24,25]. A sensitivity analysis on its outputs to different input parameters for simulating grain yield of winter wheat, water loss, GHG emissions and soil C stock has been done [26]. In this study, we use SPACSYS to assess the impact of CO₂ concentrations on crop growth, together with different climatic scenarios of shared socioeconomic pathways and hypothesise that a warming climate could enhance winter wheat and maize yield in the studied region and that SOC stocks in the topsoil and subsoil can increase in continuous monoculture systems.

2. Materials and Methods

2.1. Site Description and Experimental Design

Data used for model calibration and validation were collected from a long-term field experiment with a monoculture cropping system of winter wheat or summer maize together with treatments of chemical fertiliser only, and a combination of chemical fertiliser and manure application. The 20-year experiment was conducted in a typical tableland and gully region of the Loess Plateau, Shaanxi province, China (107°47'48" E, 35°11'57" W, ca. 1215 m a.s.l.) between 1985 and 2004 (up to 1999 for winter wheat). The climate is semi-arid and warm temperate, where the mean annual precipitation was 584 mm and the mean annual temperature was 9.3 °C over the experimental period. Monthly temperature and precipitation over the experimental period are shown in Figure 1. The soil is classified as *Cumuli-Ustic Isohumosol* soil in the Chinese soil classification, equivalent to *Udic Haplustalf* in the USDA soil taxonomy. Soil physical-chemical properties at the beginning of the experiment are given in Table 1.

As detailed descriptions of the experiment have been published elsewhere [27,29,30], it is reported here briefly. Maize was sown in mid-April and harvested in mid-September each year in each plot, while winter wheat was sown in late September each year and harvested in late June, the second year. Before sowing, plots were tilled at depths of 20 cm. Wheat and maize were irrigated at an average of 300 and 270 mm over their growing seasons, respectively. Urea was applied at the rate of 120 kg N ha⁻¹. For the combination treatment, 75,000 kg ha⁻¹ manure was added on top of the chemical fertiliser rate for each crop [31]. Each crop also received calcium superphosphate at 60 P₂O₅ kg ha⁻¹ and potassium chloride at 70 K₂O kg ha⁻¹. All fertilisers were applied before sowing. Field management, such as weed and pest control, was in accordance with local farmer practice. The plot size was 4 m × 6 m for both crops.

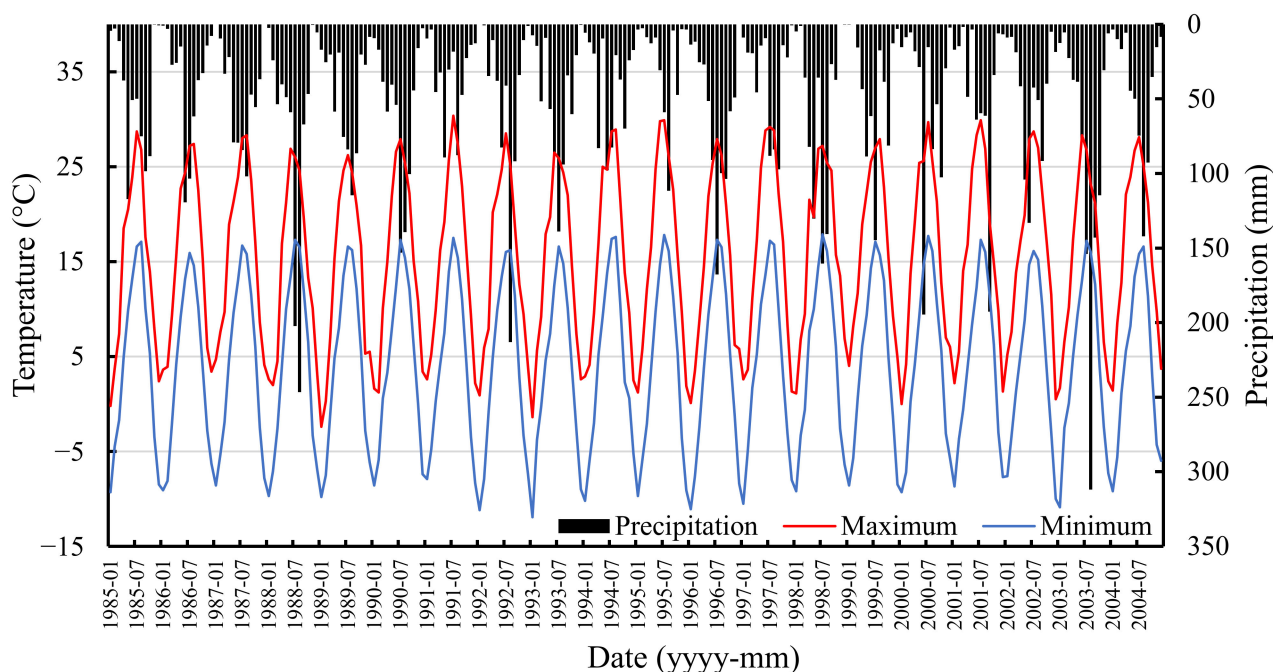


Figure 1. Monthly maximum and minimum temperatures and precipitation over the experimental period.

Table 1. Soil physical and chemical properties at the beginning of the study experiment [27,28].

| Depth (cm) | Clay (%) | Sand (%) | Silt (%) | Bulk Density (g cm ⁻³) | pH | SOC (g kg ⁻¹) | Total N (g kg ⁻¹) |
|------------|----------|----------|----------|------------------------------------|-----|---------------------------|-------------------------------|
| 0–20 | 20.6 | 10.5 | 69.0 | 1.12 | 8.3 | 6.4 | 0.98 |
| 20–40 | 18.3 | 10.6 | 71.2 | 1.06 | 8.3 | 3.8 | 0.83 |
| 40–95 | 18.2 | 10.8 | 71.0 | 1.29 | 8.3 | 3.0 | 0.61 |
| 95–150 | 19.3 | 8.1 | 72.7 | 1.4 | 8.4 | 1.9 | 0.38 |

2.2. Model Calibration and Validation

Although the SPACSYS model has been calibrated and validated for wheat and maize under various climatic and soil conditions [25,32–34], it is still important to assess its predictive performance on a study-by-study basis. For this study, the observed dataset on grain yield of wheat (1985–1999) and maize (1985–2004) was divided into two equal and sequential parts for model calibration and validation, respectively (i.e., for wheat 1985–1992 and 1993–1999, and for maize 1985–1994 and 1995–2004, respectively).

Ideally, simulated SOC dynamics should also be calibrated and validated before the model is applied for SOC prediction. Given the original purpose of the field experiment, SOC stock was not monitored. Therefore, it is impossible to validate SOC stock prediction using experimental data in this instance. However, soil C dynamics have been calibrated and validated in various cropping systems in Chinese climates and soil types [24,25], where conclusions from these previous studies gave us confidence in simulation accuracy in C cycling in this study.

2.3. Historic Weather Data and Future Climate Scenarios

Historic weather data for the study site were downloaded from the Chinese National Meteorological Information Centre (Historic weather. Available online: <http://data.cma.cn> accessed on 1 December 2021) and the product of the 6th Coupled Model Inter-Comparison Pathway (CMIP6) was used to represent future climate scenarios. CMIP6 is based on a number of shared socioeconomic pathways (SSPs) scenarios, proposed by the intergovernmental

panel on climate change (IPCC) in the 6th assessment report [13,35]. Data for six climate scenarios from 2020 to 2050 were downloaded and statistically downscaled from the UKESM1 model ($0.5 \times 0.5^\circ$) output (Climate scenario dataset: <https://www.metoffice.gov.uk> accessed on 16 December 2021) for the study site. The six climate scenarios were SSP1-1.9 and SSP1-2.6 (ssp119 and ssp126, the green road), SSP2-4.5 (ssp245, middle of the road), SSP3-7.0 (ssp370, a rocky road by regional rivalry), SSP4-3.4 (ssp434, a divided road by inequality) and SSP5-8.5 (ssp585, the highway by fossil-fuelled development) [36,37]. Each CMIP6 output dataset is distinguished with the variant-id global attribute of r1i1p1f, r2i1p1f, r3i1p1f, r4i1p1f and r8i1p1f, where the numbers are indices for a particular configuration of the realisation (i.e., ensemble member), initialisation method, physics and forcing (VARIANT-ID IN CMIP6 METADATA. <https://ukesm.ac.uk/cmip6/variant-id/> accessed on 16 December 2021 for details). For this study, datasets with all five realisations under each climate scenario were used so as to reduce bias in the UKESM1 model output.

2.4. Simulation Configuration under Six Climate Scenarios

For this study, the focus was on the simulation of crop yield and soil C storage to dis-entangle the causes of crop failure for the given future climate scenarios, and in turn, to assess the impacts of climate change on crop productivity. The SPACSYS model was run for each climate scenario and specified with the same agronomic practices as the study plot experiment in terms of cultivar, sowing dates, tillage, irrigation and fertiliser applications. The crops were harvested at maturity as determined by the algorithm implemented in SPACSYS. Decadal climate conditions under the six climatic scenarios over the crop growing seasons for wheat and maize are shown in Figure 2.

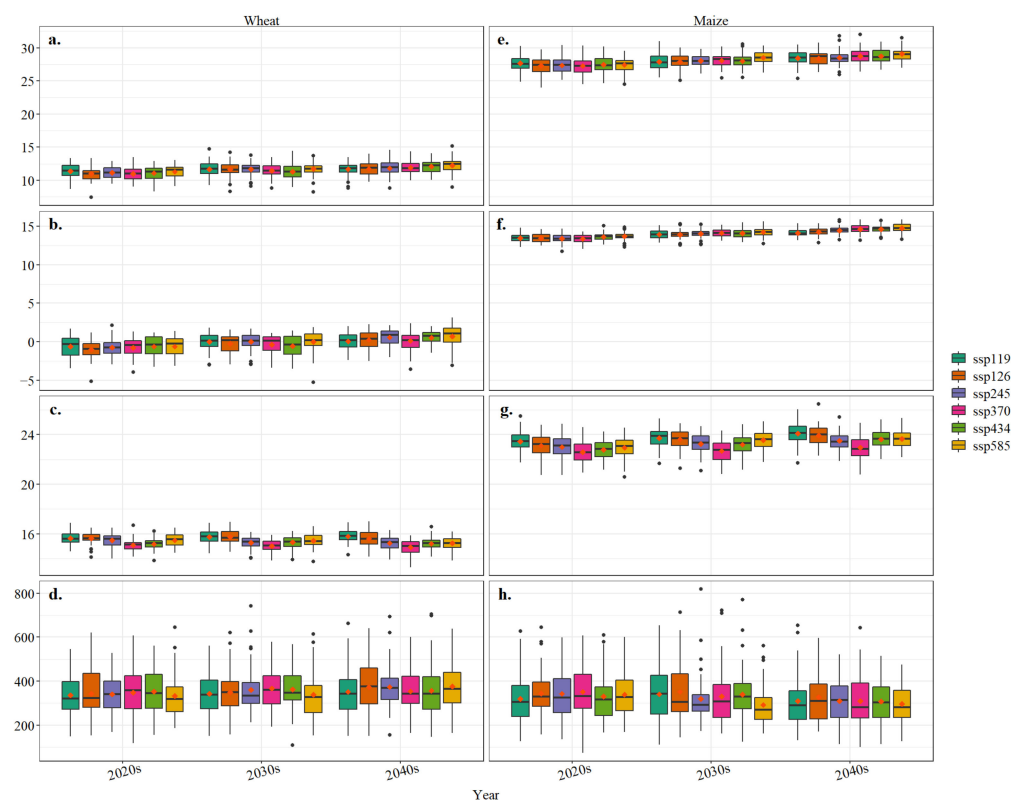


Figure 2. Down-scaled average decadal maximum (T_{max}) and minimum (T_{min}) temperatures, solar radiation (Rad) and precipitation (Pr) for the six climate scenarios over the crop growing seasons of winter wheat (a–d) and maize (e–h).

2.5. Crop Failure Rate

The crop failure rate defined by the ratio of the frequency for a crop yield below a set threshold to the total harvest time over a given time period, was used to assess the impacts

of climatic conditions on crop yield. For this study, the threshold was set as one standard deviation below the mean over the given time period [38,39].

2.6. Statistical Analysis for Model Performance

To investigate SPACSYS accuracy in simulating wheat and maize yields, the following six model performance indices were used: the model efficiency (EF), the coefficient of determination (CD) [40], the normalised root mean squared error (nRMSE), the correlation coefficient (r), the relative error (RE) and the mean difference (MD). Their calculation formulae are shown in Table 2, along with minimum, maximum and ideal (perfect model accuracy) values. One-way ANOVA and the least significant difference (LSD, $p < 0.05$) method were used to test the significance of climate effects on average values of grain yield of wheat and maize, and soil C stocks, respectively. The analyses were conducted using SPSS 20.0 (SPSS, Inc., 2011, Chicago, IL, USA).

Table 2. Accuracy indices formulae, where O_i is the observed value of the i th sample, S_i is the simulated value, \bar{O} is the mean of the observed data, \bar{S} is the mean of the simulated data, and n is the number of paired values.

| Item | Formula | Minimum | Maximum | Ideal Value |
|-------|-----------------------------------------------------------------------------------------------------------------------------------------|-----------|----------|-------------|
| r | $r = \frac{\sum_{i=1}^n (O_i - \bar{O})(S_i - \bar{S})}{(\sum_{i=1}^n (O_i - \bar{O})^2)^{1/2} (\sum_{i=1}^n (S_i - \bar{S})^2)^{1/2}}$ | -1 | 1 | 1 |
| nRMSE | $\text{nRMSE} = \frac{100}{\bar{O}} \sqrt{\sum_{i=1}^n (S_i - O_i)^2 / n}$ | $-\infty$ | ∞ | 0 |
| EF | $\text{EF} = \frac{(\sum_{i=1}^n (O_i - \bar{O})^2 - \sum_{i=1}^n (S_i - O_i)^2)}{\sum_{i=1}^n (O_i - \bar{O})^2}$ | $-\infty$ | 1 | 1 |
| CD | $\text{CD} = \frac{\sum_{i=1}^n (O_i - \bar{O})^2}{\sum_{i=1}^n (S_i - \bar{O})^2}$ | $-\infty$ | ∞ | 1 |
| MD | $\text{MD} = \sum_{i=1}^n (O_i - S_i) / n$ | $-\infty$ | ∞ | 0 |
| RE | $\text{RE} = \frac{100}{n} \sum_{i=1}^n (S_i - O_i) / O_i$ | $-\infty$ | ∞ | 0 |

3. Results

3.1. Model Performance

Visual comparisons between simulated and observed wheat and maize grain yields over the 20-year experimental period are shown in Figure 3 together with model performance indices in Table 3 for separate calibration and validation datasets. Visually, the pattern and magnitude of simulated grain yield agreed well with the observed values. Simulated wheat yield tended to capture the high observed peaks but tended to over-predict over the entire period (Figure 3a), which was confirmed by negative values of the accuracy index (MD) in Table 3. Conversely, simulated maize did not capture the observed unusually low yields in 1997 and 2004 (Figure 3b) but tended to under-predict over the entire period (i.e., positive values of MD in Table 3). For the entire period, simulated grain yield for wheat was over-predicted by 17.3% while for maize, it was under-predicted by 6.3%. As would be expected, all model performance indices showed a decrease in model accuracy moving from the calibration to validation datasets (Table 3). The statistical results confirmed that the correlations between simulated and observed data indicated reasonably accurate model performance as all $r > 0.6$. Further, all $\text{EF} > 0$ and three of the four $\text{CD} > 1$ which indicated the simulated values could estimate the trend in the observed data more accurately than that in observed mean. In summary, the results suggested that the SPACSYS model could provide reasonably accurate yield predictions for both crops.

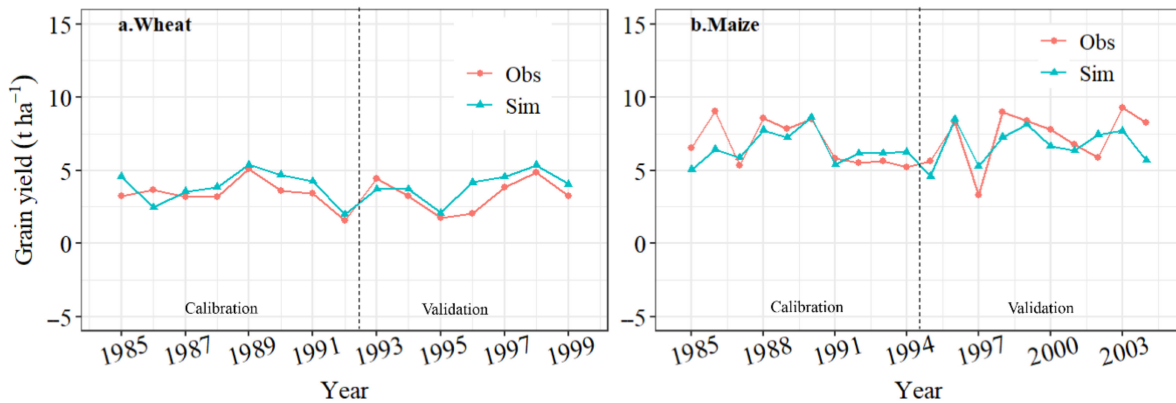


Figure 3. Simulated (blue line) and observed (red line) yields for wheat (a) and maize (b) over the simulation period.

Table 3. Model evaluation diagnostics for simulated yield of wheat and maize.

| Index ¹ | Wheat | | Maize | |
|--------------------|-------------|------------|-------------|------------|
| | Calibration | Validation | Calibration | Validation |
| r | 0.75 | 0.71 | 0.67 | 0.64 |
| nRMSE | 25.66 | 29.37 | 16.39 | 19.95 |
| EF | 0.06 | 0.14 | 0.40 | 0.33 |
| CD | 0.68 | 1.30 | 1.97 | 2.10 |
| MD | −0.48 | −0.61 | 0.31 | 0.49 |
| RE | −14.2 | −18.2 | 4.6 | 6.7 |
| N | 8 | 7 | 10 | 10 |

¹ r : the correlation coefficient; nRMSE, the normalised root mean squared error; EF: the model efficiency; CD: the coefficient of determination; MD: the mean difference; RE: the relative error; and n : the number of sampled and simulated pairs.

3.2. Simulated Crop Failure under Climate Change

The crop failure rate of wheat and maize varied with six future climate scenarios (Figure 4). Compared to the baseline (historical), the failure rate for wheat tended to decline over time for five of the six climate scenarios except ssp585 (the highway by fossil-fuelled development) under which the failure rate tended to increase (Figure 4a). This implies that climate change may be favourable for wheat production. However, the reverse was found for maize, where failure rate increased under all six climate scenarios, especially, during the last decadal period (2040–2049) where it was approximately twofold of that during the first decadal period (2020–2029) (Figure 4b).

3.3. Climate Change Impact on Grain Yield

The future trends (2020–2049) in predicted grain yield of wheat and maize are shown in Figure 5. Compared with an average yield under the baseline, wheat yield under all six climate scenarios would increase from between 194 to 664 kg ha^{−1}, while maize yield would decline from between 220 and 1807 kg ha^{−1}. In general, wheat yield would increase year-on-year under low emission scenarios (ssp119, ssp126, ssp245 and ssp370) but would decline year-on-year under high emission scenarios (ssp434 and ssp585) (Figure 5a). However, maize yield would decline year-on-year with all six emission intensity scenarios (Figure 5b).

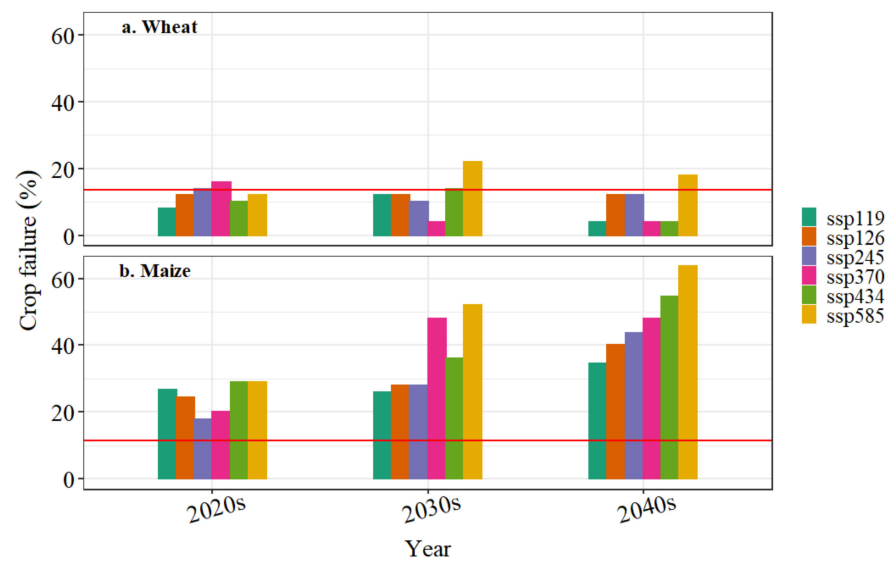


Figure 4. Crop failure rate for wheat (a) and maize (b) compared with the historical failure percentage (red line) under the six climate change scenarios.

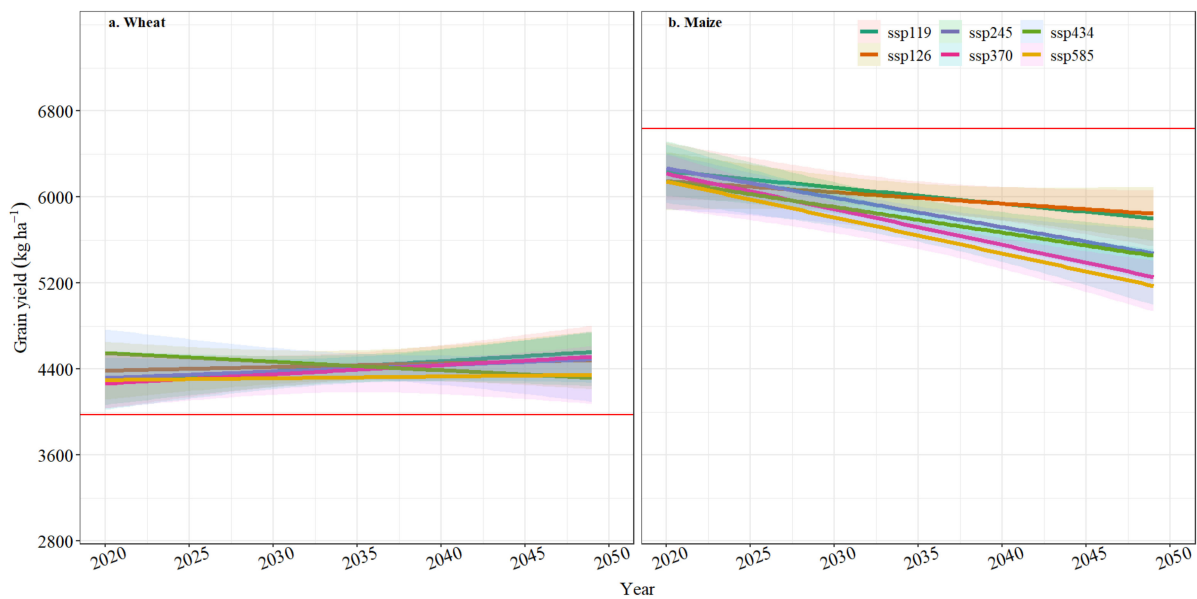


Figure 5. Trends in wheat (a) and maize (b) grain yield from the six climate change scenarios between 2020 to 2049 compared with the average under the baseline (red horizontal line). The shadow of each line for each climate scenario represents 95% confidence interval of predicted yield with five ensembled member datasets.

3.4. Simulated SOC Stocks in the Topsoil and Subsoil

Climate change and agronomic practices could lead to significant effects on the SOC pool (Figure 6). The lowest values of simulated SOC stocks in the wheat and maize fields occurred under the ssp585 scenario, especially over the period of 2040–2049. Low emission scenarios such as ssp119, ssp126 and ssp245 tended to increase SOC. During 2040–2049, SOC stocks for each scenario are in the following order: ssp126 \approx ssp119 > ssp245 > ssp585 \approx ssp370 > ssp434 for wheat and ssp126 \approx ssp119 > ssp245 > ssp370 > ssp434 > ssp585 for maize. SOC content in the top 30 cm soil layer in both wheat and maize fields would increase over time (Figure 6a,b) but would decrease in the subsoil (30–100 cm). The lowest SOC stock in the subsoil was found under the ssp585 scenario (Figure 6c,d). Relative to the average under the baseline, topsoil SOC stocks in the wheat fields under six climate

scenarios increased between 3.8 and 35.2%, while SOC stocks in the maize fields both decreased and increased (between -5.0 and 10.1%) relative to the baseline.

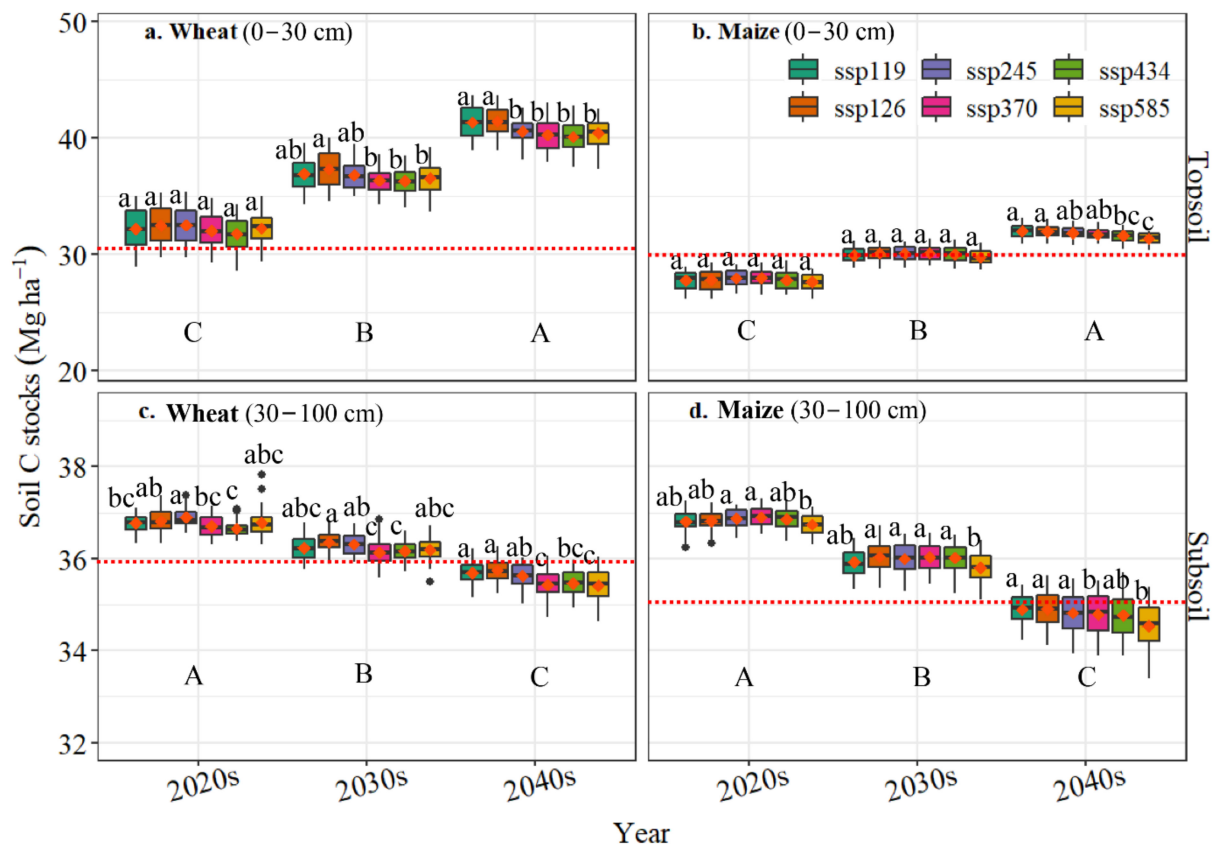


Figure 6. Boxplots summarizing decadal variations in simulated SOC stocks in the wheat (a,c) and maize (b,d) fields under six climate scenarios (ssp119, ssp126, ssp245, ssp370, ssp434 and ssp585) for the 0–30 cm (topsoil) and 30–100 cm (subsoil) layers during 2020–2049. Baseline historical data is given as dashed red horizontal lines. For each boxplot, the central mark is the median, the red square indicates the mean value, the edges of the box are the 25th and 75th percentiles, and the whiskers extend to the extreme data points not considered to be outliers. Extremes are indicated by both minimum and maximum values (filled circles). Different lowercase letters represent significant differences ($p < 0.05$) under different climate scenarios in each time slice. Different capital letters represent significant differences ($p < 0.05$) between time slices under the six climate scenarios.

4. Discussion

4.1. Climate Change Impacts on Grain Yield and Crop Failure

Study simulation results indicated that grain yield for both wheat and maize will be impacted by climate change in the Loess area, which agrees with previous studies [27,41]. However, the extent of the projected climate impacts is different between the cropping systems. For the continuous wheat cropping system, climate change will tend to have positive impacts on grain yield trends except under climate scenario ssp434 (a divided road by inequality). Trends are in agreement with conclusions in a meta-analysis on winter wheat yield in a world under the condition of higher atmospheric CO₂ concentrations and without drastic decrease in precipitation [42], which is a similar configuration (less or no water stress because of irrigation) to that used in our simulations. Increasing temperatures at the early vegetative stage results in a prolonged vernalisation process for the over-winter crop, leading to reduced grain quality and yield [43]. Under scenario ssp585, the average minimum and maximum air temperatures during the 2040s increased by 1.3 and 0.9 °C, respectively, compared with those during the 2020s. If precipitation decreases, then the yield will drop dramatically [21], as possibly reflected in our simulation under scenario ssp434.

The distribution of rainfall under scenario ssp434 shifted over the growing period (Figure 2) whilst the irrigation schedules were fixed to be the same as that used in experimental practice. Further, there were differences in the temporal patterns of precipitation between the chosen scenarios and the temporal patterns observed in the historic records (during the experimental years). Therefore, there could be water stress in some growing seasons of winter wheat. For future studies, irrigation schedules should be adjusted based on precipitation and soil water content. For the continuous maize cropping system, the predicted maize yield declined under all six scenarios (Figure 5b). Compared with the average of the historical yield, maize yield would decrease by 4.2–16.7% under the six scenarios. This agrees with previous studies in that it will decrease by 9% and 24% in the American Corn Belt and in China due to future global warming [44,45]. In contrast to winter wheat, higher temperatures speed up phenological development of maize. Shorter growing seasons under the likely warming conditions together with expected lower solar radiation (Figure 2g) causes yield decrease even with the increased atmospheric CO₂ concentrations. Here, it should be noted however, that predicted crop yields using different agricultural models with weather data generated from different climate models might be incompatible with respect to yield uncertainties or variances, although broad trends in yield should be similar.

Under climate change, the grain yield of both crops could become more unstable in the Loess region (Figures 4 and 5). Compared with the experimental yields, the crop failure rate for maize increased between 6.4–52.2% but decreased for wheat (except under scenario ssp585). This agrees with previous studies that forecasted increases in cereal crop failures with increases in temperature [5,46]. Although, it has also been reported that CO₂ effects could largely overcome the failure risks attributable to increases in temperature [47]. Apart from heat stress or shorter growing periods, further influence could be due to improper or unbalanced inorganic fertiliser applications [34], where in our simulations, the impacts of nitrogen on crop growth and yields were included. As with previous and any model-based study, results (crop failure rates) depend on model assumptions and should be interpreted in this context. For example, we assumed that the crop cultivars and agronomic management practices do not change, and that the sowing dates of the crops are fixed over the whole simulation period. In reality however, adaptation to climate change or weather variability would likely be taken. For example, wheat cultivars that are insensitive to vernalisation might be selected for warming winters and where sowing dates are determined by soil temperature and water availability each year. Clearly, if adaptation strategies were considered, then the crop failure rate would likely reduce.

4.2. Climate Change Impacts on SOC Stocks

Given there were no data for SOC stock from the experiments, our simulations for soil C cycling could not be assessed for their accuracy. However, the average of the simulated annual SOC stocks under the baseline period is within the reported range (18–50 Mg C ha⁻¹) [34]. Furthermore, climate change is expected to have negative impacts on SOC stocks for cereal crop fields [48–51], which is supported by our study. Compared with the highest average SOC stock among the six scenarios, at each time slice, SOC stocks in the wheat field under the scenarios decreased by 8.1–132.3 Mg C ha⁻¹ for the topsoil zone and by 5.6–32.6 Mg C ha⁻¹ for the subsoil zone (Figure 6a,c). Similarly, the average stocks in the maize field decreased by 5.6–64.6 Mg C ha⁻¹ and 1.2–37.1 Mg C ha⁻¹ for topsoil and subsoil zones, respectively (Figure 6b,d). Interestingly, however, predicted SOC stocks in the topsoil layer in both fields significantly increased while it decreased in the subsoil layer compared with that during the experimental years. This might be a consequence of the contributions from crop residue and roots to the topsoil rather than to the subsoil as wheat and maize roots predominately sit in the topsoil layer [52–54]. Soil organic C is lost through the decomposition process that is controlled by soil temperature, moisture, quality of organic matter, ammonium content and microbial biomass. Higher soil temperatures under the warming scenarios can prompt soil microbial activities given no other limitations exist.

Counteracting higher temperatures, appropriate soil moisture and ammonium presence through chemical fertiliser application in the topsoil layer, entails the addition of crop residue and roots will compensate C loss through decomposition. Conversely, the subsoil zone is more susceptible to nutrient input, and fresh plant-derived C to the subsoil layer stimulates recalcitrant soil organic matter degradation, which could decrease SOC stock in the subsoil due to the priming effects [55,56].

5. Conclusions

In this study, the SPACSYS model together with climatic products from the UKESM1 model under CMIP6 was used to simulate potential impacts of climate change on crop productivity and SOC dynamics for both winter wheat and maize in northern China. Warming scenarios appeared favourable for reducing crop failure and increasing the grain yield of winter wheat but appeared detrimental to maize even with irrigation. A continuous monoculture cropping system was projected to increase C content in the arable topsoil layer. Irrigation was found to play a critical role in crop failure decline and would be transferrable to regions under similar climates. Thus, strategies for water allocation at a regional level for agricultural consumption should be developed to maintain crop production under climate change along with possible sustainable agronomic practices in the future.

Author Contributions: Conceptualisation, L.W., P.H., M.H., K.G. and H.Y.; software, L.W.; validation, K.G. and H.Y.; formal analysis, C.L.; data curation, M.H. and L.W.; writing—original draft preparation, C.L.; writing—review and editing, ALL; visualisation, C.L.; supervision, L.W.; funding acquisition, L.W. All authors have read and agreed to the published version of the manuscript.

Funding: This work was supported by the Natural Environment Research Council (NE/N007433/1 and NE/S009094/1).

Institutional Review Board Statement: Not applicable.

Informed Consent Statement: Not applicable.

Data Availability Statement: The data presented in this study are openly available in NERC EDS Environmental Information Data Centre at <https://doi.org/10.5285/03e74f94-88a5-4f09-b9ea-1447dd3e2b85>, accessed on 23 April 2022.

Conflicts of Interest: The authors declare no conflict of interest.

References

1. Rosenzweig, C.; Elliott, J.; Deryng, D.; Ruane, A.C.; Müller, C.; Arneth, A.; Boote, K.J.; Folberth, C.; Glotter, M.; Khabarov, N.; et al. Assessing agricultural risks of climate change in the 21st century in a global gridded crop model intercomparison. *Proc. Natl. Acad. Sci. USA* **2014**, *111*, 3268. [[CrossRef](#)] [[PubMed](#)]
2. Porter, J.R.; Challinor, A.J.; Henriksen, C.B.; Howden, S.M.; Martre, P.; Smith, P. Invited review: Intergovernmental Panel on Climate Change, agriculture, and food—A case of shifting cultivation and history. *Glob. Chang. Biol.* **2019**, *25*, 2518–2529. [[CrossRef](#)] [[PubMed](#)]
3. Hatfield, J.L.; Prueger, J.H. Temperature extremes: Effect on plant growth and development. *Weather Clim. Extrem.* **2015**, *10*, 4–10. [[CrossRef](#)]
4. Hoegh-Guldberg, O.; Jacob, D.; Taylor, M.; Guillén Bolaños, T.; Bindi, M.; Brown, S.; Camilloni, I.A.; Diedhiou, A.; Djalante, R.; Ebi, K.; et al. The human imperative of stabilizing global climate change at 1.5 °C. *Science* **2019**, *365*, eaaw6974. [[CrossRef](#)] [[PubMed](#)]
5. Gaupp, F.; Hall, J.; Mitchell, D.; Dadson, S. Increasing risks of multiple breadbasket failure under 1.5 and 2 °C global warming. *Agric. Syst.* **2019**, *175*, 34–45. [[CrossRef](#)]
6. Li, Y.; Guan, K.; Schnitkey, G.D.; DeLucia, E.; Peng, B. Excessive rainfall leads to maize yield loss of a comparable magnitude to extreme drought in the United States. *Glob. Chang. Biol.* **2019**, *25*, 2325–2337. [[CrossRef](#)] [[PubMed](#)]
7. Liu, C.; Wang, L.; Cocq, K.L.; Chang, C.; Li, Z.; Chen, F.; Liu, Y.; Wu, L. Climate change and environmental impacts on and adaptation strategies for production in wheat-rice rotations in southern China. *Agric. For. Meteorol.* **2020**, *292–293*, 108136. [[CrossRef](#)]
8. Jin, Z.; Ainsworth, E.A.; Leakey, A.D.B.; Lobell, D.B. Increasing drought and diminishing benefits of elevated carbon dioxide for soybean yields across the US Midwest. *Glob. Chang. Biol.* **2018**, *24*, e522–e533. [[CrossRef](#)] [[PubMed](#)]
9. Singer, S.D.; Soolanayakanahally, R.Y.; Foroud, N.A.; Kroebe, R. Biotechnological strategies for improved photosynthesis in a future of elevated atmospheric CO₂. *Planta* **2019**, *251*, 24. [[CrossRef](#)]

10. Chen, Y.; Zhang, Y.; Chen, N.; Cong, N.; Zhu, J.; Zhao, G.; Zu, J.; Liu, Y.; Zhu, Y.; Zheng, Z.; et al. Nitrogen availability and precipitation variability regulated CO₂ fertilization effects on carbon fluxes in an alpine grassland. *Agric. For. Meteorol.* **2021**, *307*, 108524. [[CrossRef](#)]
11. Kalra, N.; Chander, S.; Pathak, H.; Aggarwal, P.K.; Gupta, N.C.; Sehgal, M.; Chakraborty, D. Impacts of climate change on agriculture. *Outlook Agric.* **2007**, *36*, 109–118. [[CrossRef](#)]
12. Lefèvre, C.; Rekik, F.; Alcantara, V.; Wiese, L. *Soil Organic Carbon: The Hidden Potential*; Food and Agriculture Organization of the United Nations (FAO): Rome, Italy, 2017.
13. IPCC. *Climate Change and Land: An IPCC Special Report on Climate Change, Desertification, Land Degradation, Sustainable Land Management, Food Security, and Greenhouse Gas Fluxes in Terrestrial Ecosystems*; Shukla, P.R., Skea, J., Buendia, E.C., Masson-Delmotte, V., Pörtner, H.-O., Roberts, D.C., Zhai, P., Slade, R., Connors, S., van Diemen, R., et al., Eds.; Intergovernmental Panel on Climate Change (IPCC): Geneva, Switzerland, 2019.
14. Yao, Y.; Dai, Q.; Gao, R.; Gan, Y.; Yi, X. Effects of rainfall intensity on runoff and nutrient loss of gently sloping farmland in a karst area of SW China. *PLoS ONE* **2021**, *16*, e0246505. [[CrossRef](#)] [[PubMed](#)]
15. Cotrufo, M.F.; Del Galdo, I.; Piermatteo, D. Litter decomposition: Concepts, methods and future perspectives. In *Soil Carbon Dynamics: An Integrated Methodology*; Kutsch, W., Bahn, M., Heinemeyer, A., Eds.; Cambridge University Press: Cambridge, UK, 2010; pp. 76–90. [[CrossRef](#)]
16. Wu, W.; Tang, H.; Yang, P.; You, L.; Zhou, Q.; Chen, Z.; Shibasaki, R. Scenario-based assessment of future food security. *J. Geogr. Sci.* **2011**, *21*, 3–17. [[CrossRef](#)]
17. Ding, Y.-J.; Li, C.-Y.; Wang, X.; Wang, Y.; Wang, S.-X.; Chang, Y.-P.; Qin, J.; Wang, S.-P.; Zhao, Q.-D.; Wang, Z.-R. An overview of climate change impacts on the society in China. *Adv. Clim. Chang. Res.* **2021**, *12*, 210–223. [[CrossRef](#)]
18. Xie, W.; Huang, J.; Wang, J.; Cui, Q.; Robertson, R.; Chen, K. Climate change impacts on China's agriculture: The responses from market and trade. *China Econ. Rev.* **2020**, *62*, 101256. [[CrossRef](#)]
19. Jones, J.W.; Antle, J.M.; Basso, B.; Boote, K.J.; Conant, R.T.; Foster, I.; Godfray, H.C.J.; Herrero, M.; Howitt, R.E.; Janssen, S.; et al. Brief history of agricultural systems modeling. *Agric. Syst.* **2017**, *155*, 240–254. [[CrossRef](#)]
20. Wu, L.; McGechan, M.; McRoberts, N.; Baddeley, J.; Watson, C. SPACSYS: Integration of a 3D root architecture component to carbon, nitrogen and water cycling—Model description. *Ecol. Model.* **2007**, *200*, 343–359. [[CrossRef](#)]
21. Pirttioja, N.; Carter, T.R.; Fronzek, S.; Bindi, M.; Hoffmann, H.; Palosuo, T.; Ruiz-Ramos, M.; Tao, F.; Trnka, M.; Acutis, M.; et al. Temperature and precipitation effects on wheat yield across a European transect: A crop model ensemble analysis using impact response surfaces. *Clim. Res.* **2015**, *65*, 87–105. [[CrossRef](#)]
22. Wu, L.; Blackwell, M.; Dunham, S.; Hernández-Allica, J.; McGrath, S.P. Simulation of phosphorus chemistry, uptake and utilisation by winter wheat. *Plants* **2019**, *8*, 404. [[CrossRef](#)]
23. Wu, L.; Harris, P.; Misselbrook, T.; Lee, M. Simulating grazing beef and sheep systems. *Agric. Syst.* **2022**, *195*, 103307. [[CrossRef](#)]
24. Zhang, X.; Xu, M.; Sun, N.; Xiong, W.; Huang, S.; Wu, L. Modelling and predicting crop yield, soil carbon and nitrogen stocks under climate change scenarios with fertiliser management in the North China Plain. *Geoderma* **2016**, *265*, 176–186. [[CrossRef](#)]
25. Zhang, X.; Sun, Z.; Liu, J.; Ouyang, Z.; Wu, L. Simulating greenhouse gas emissions and stocks of carbon and nitrogen in soil from a long-term no-till system in the North China Plain. *Soil Tillage Res.* **2018**, *178*, 32–40. [[CrossRef](#)]
26. Shan, Y.; Huang, M.B.; Harris, P.; Wu, L.H. A sensitivity analysis of the SPACSYS model. *Agriculture* **2021**, *11*, 624. [[CrossRef](#)]
27. Huang, M.; Gallichand, J.; Dang, T.; Shao, M. An evaluation of EPIC soil water and yield components in the gully region of Loess Plateau, China. *J. Agric. Sci.* **2006**, *144*, 339–348. [[CrossRef](#)]
28. Chen, H.; Zhao, Y.; Feng, H.; Li, H.; Sun, B. Assessment of climate change impacts on soil organic carbon and crop yield based on long-term fertilization applications in Loess Plateau, China. *Plant Soil* **2015**, *390*, 401–417. [[CrossRef](#)]
29. Chen, H.; Shao, M.; Li, Y. The characteristics of soil water cycle and water balance on steep grassland under natural and simulated rainfall conditions in the Loess Plateau of China. *J. Hydrol.* **2008**, *360*, 242–251. [[CrossRef](#)]
30. Yi, L.; Shenjiao, Y.; Shiqing, L.; Xinping, C.; Fang, C. Growth and development of maize (*Zea mays* L.) in response to different field water management practices: Resource capture and use efficiency. *Agric. For. Meteorol.* **2010**, *150*, 606–613. [[CrossRef](#)]
31. Huang, M.; Dang, T.; Gallichand, J.; Goulet, M. Effect of increased fertilizer applications to wheat crop on soil-water depletion in the Loess Plateau, China. *Agric. Water Manag.* **2003**, *58*, 267–278. [[CrossRef](#)]
32. Liang, S.; Li, Y.; Zhang, X.; Sun, Z.; Sun, N.; Duan, Y.; Xu, M.; Wu, L. Response of crop yield and nitrogen use efficiency for wheat-maize cropping system to future climate change in northern China. *Agric. For. Meteorol.* **2018**, *262*, 310–321. [[CrossRef](#)]
33. Liang, S.; Zhang, X.; Sun, N.; Li, Y.; Xu, M.; Wu, L. Modeling crop yield and nitrogen use efficiency in wheat and maize production systems under future climate change. *Nutr. Cycl. Agroecosys* **2019**, *115*, 117–136. [[CrossRef](#)]
34. Zhang, X.; Sun, N.; Wu, L.; Xu, M.; Bingham, I.J.; Li, Z. Effects of enhancing soil organic carbon sequestration in the topsoil by fertilization on crop productivity and stability: Evidence from long-term experiments with wheat-maize cropping systems in China. *Sci. Total Environ.* **2016**, *562*, 247–259. [[CrossRef](#)] [[PubMed](#)]
35. Reimann, L.; Vollstedt, B.; Koerth, J.; Tsakiris, M.; Beer, M.; Vafeidis, A.T. Extending the Shared Socioeconomic Pathways (SSPs) to support local adaptation planning—A climate service for Flensburg, Germany. *Futures* **2021**, *127*, 102691. [[CrossRef](#)]
36. Frame, B.; Lawrence, J.; Ausseil, A.-G.; Reisinger, A.; Daigneault, A. Adapting global shared socio-economic pathways for national and local scenarios. *Clim. Risk Manag.* **2018**, *21*, 39–51. [[CrossRef](#)]

37. O'Neill, B.C.; Carter, T.R.; Ebi, K.; Harrison, P.A.; Kemp-Benedict, E.; Kok, K.; Kriegler, E.; Preston, B.L.; Riahi, K.; Sillmann, J.; et al. Achievements and needs for the climate change scenario framework. *Nat. Clim. Chang.* **2020**, *10*, 1074–1084. [[CrossRef](#)]
38. Parkes, B.; Challinor, A.; Nicklin, K. Crop failure rates in a geoengineered climate: Impact of climate change and marine cloud brightening. *Environ. Res. Lett.* **2015**, *10*, 084003. [[CrossRef](#)]
39. Yang, H.; Dobbie, S.; Ramirez-Villegas, J.; Chen, B.; Qiu, S.; Ghosh, S.; Challinor, A. South India projected to be susceptible to high future groundnut failure rates for future climate change and geo-engineered scenarios. *Sci. Total Environ.* **2020**, *747*, 141240. [[CrossRef](#)] [[PubMed](#)]
40. Loague, K.; Green, R.E. Statistical and graphical methods for evaluating solute transport models: Overview and application. *J. Contam. Hydrol.* **1991**, *7*, 51–73. [[CrossRef](#)]
41. Xiao, D.; Liu, D.L.; Feng, P.; Wang, B.; Waters, C.; Shen, Y.; Qi, Y.; Bai, H.; Tang, J. Future climate change impacts on grain yield and groundwater use under different cropping systems in the North China Plain. *Agric. Water Manag.* **2021**, *246*, 106685. [[CrossRef](#)]
42. Wilcox, J.; Makowski, D. A meta-analysis of the predicted effects of climate change on wheat yields using simulation studies. *Field Crops Res.* **2014**, *156*, 180–190. [[CrossRef](#)]
43. Rezaei, E.E.; Siebert, S.; Hüging, H.; Ewert, F. Climate change effect on wheat phenology depends on cultivar change. *Sci. Rep.* **2018**, *8*, 4891. [[CrossRef](#)]
44. Izaurralde, R.C.; Rosenberg, N.J.; Brown, R.A.; Thomson, A.M. Integrated assessment of Hadley Center (HadCM2) climate-change impacts on agricultural productivity and irrigation water supply in the conterminous United States: Part II. Regional agricultural production in 2030 and 2095. *Agric. For. Meteorol.* **2003**, *117*, 97–122. [[CrossRef](#)]
45. Li, R.; Zheng, J.; Xie, R.; Ming, B.; Peng, X.; Luo, Y.; Zheng, H.; Sui, P.; Wang, K.; Hou, P.; et al. Potential mechanisms of maize yield reduction under short-term no-tillage combined with residue coverage in the semi-humid region of Northeast China. *Soil Tillage Res.* **2022**, *217*, 105289. [[CrossRef](#)]
46. Challinor, A.J.; Simelton, E.S.; Fraser, E.D.G.; Hemming, D.; Collins, M. Increased crop failure due to climate change: Assessing adaptation options using models and socio-economic data for wheat in China. *Environ. Res. Lett.* **2010**, *5*, 034012. [[CrossRef](#)]
47. Ruane, A.C.; Antle, J.; Elliott, J.; Folberth, C.; Hoogenboom, G.; Mason-D'Croz, D.; Müller, C.; Porter, C.; Phillips, M.M.; Raymundo, R.M.; et al. Biophysical and economic implications for agriculture of +1.5° and +2.0 °C global warming using AgMIP Coordinated Global and Regional Assessments. *Clim. Res.* **2018**, *76*, 17–39. [[CrossRef](#)] [[PubMed](#)]
48. Börjesson, G.; Bolinder, M.A.; Kirchmann, H.; Kätterer, T. Organic carbon stocks in topsoil and subsoil in long-term ley and cereal monoculture rotations. *Biol. Fertil. Soils* **2018**, *54*, 549–558. [[CrossRef](#)]
49. Qiu, L.; Hao, M.; Wu, Y. Potential impacts of climate change on carbon dynamics in a rain-fed agro-ecosystem on the Loess Plateau of China. *Sci. Total Environ.* **2017**, *577*, 267–278. [[CrossRef](#)]
50. Thomson, A.M.; Izaurralde, R.C.; Rosenberg, N.J.; He, X. Climate change impacts on agriculture and soil carbon sequestration potential in the Huang-Hai Plain of China. *Agric. Ecosyst. Environ.* **2006**, *114*, 195–209. [[CrossRef](#)]
51. Álvaro-Fuentes, J.; Easter, M.; Cantero-Martinez, C.; Paustian, K. Modelling soil organic carbon stocks and their changes in the northeast of Spain. *Eur. J. Soil Sci.* **2011**, *62*, 685–695. [[CrossRef](#)]
52. Hirte, J.; Leifeld, J.; Abiven, S.; Mayer, J. Maize and wheat root biomass, vertical distribution, and size class as affected by fertilization intensity in two long-term field trials. *Field Crops Res.* **2018**, *216*, 197–208. [[CrossRef](#)]
53. Wang, C.; Liu, W.; Li, Q.; Ma, D.; Lu, H.; Feng, W.; Xie, Y.; Zhu, Y.; Guo, T. Effects of different irrigation and nitrogen regimes on root growth and its correlation with above-ground plant parts in high-yielding wheat under field conditions. *Field Crops Res.* **2014**, *165*, 138–149. [[CrossRef](#)]
54. Chen, X.; Zhang, J.; Chen, Y.; Li, Q.; Chen, F.; Yuan, L.; Mi, G. Changes in root size and distribution in relation to nitrogen accumulation during maize breeding in China. *Plant Soil* **2014**, *374*, 121–130. [[CrossRef](#)]
55. Fontaine, S.; Barot, S.; Barré, P.; Bdioui, N.; Mary, B.; Rumpel, C. Stability of organic carbon in deep soil layers controlled by fresh carbon supply. *Nature* **2007**, *450*, 277–280. [[CrossRef](#)] [[PubMed](#)]
56. Salomé, C.; Nunan, N.; Pouteau, V.; Lerch, T.Z.; Chenu, C. Carbon dynamics in topsoil and in subsoil may be controlled by different regulatory mechanisms. *Glob. Chang. Biol.* **2010**, *16*, 416–426. [[CrossRef](#)]